ACS Catalysis

Research Article

pubs.acs.org/acscatalysis

Origins of Stereoselectivity in Peptide-Catalyzed Kinetic Resolution of Alcohols

Rong-Zhen Liao,*[,†] Stefano Santoro,*[,‡] Martin Gotsev,[§] Tommaso Marcelli,[§] and Fahmi Himo*[,§]

[†]Key Laboratory of Material Chemistry for Energy Conversion and Storage, Ministry of Education, School of Chemistry and Chemical Engineering, Huazhong University of Science and Technology, Wuhan 430074, People's Republic of China

[‡]Department of Chemistry, Biology and Biotechnology, University of Perugia, Via Elce di Sotto 8, 06123 Perugia, Italy

[§]Department of Organic Chemistry, Arrhenius Laboratory, Stockholm University, SE-106 91 Stockholm, Sweden

Supporting Information

ABSTRACT: The origin of the stereoselectivity of the tetrapeptide-catalyzed kinetic resolution of *trans*-2-*N*-acetamidocyclohexanol is investigated by means of density functional theory calculations. Transition states for the functionalization of both (*R*,*R*) and (*S*,*S*) substrates were optimized considering all possible conformers. Due to the flexibility of the peptidic catalyst, a large number of transition states had to be located, and analysis of the geometries and energies allowed for the identification of the main factors that control the stereoselectivity.

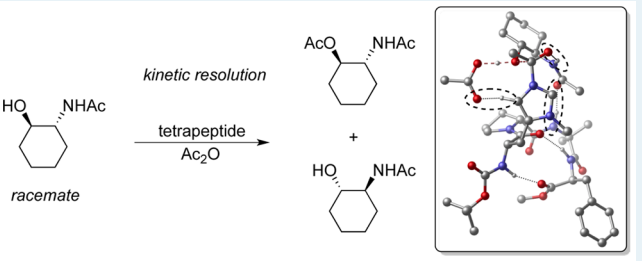

KEYWORDS: *organocatalysis, enantioselectivity, acylation, density functional theory, transition state, reaction mechanism*

1. INTRODUCTION

Enzymes have always been a source of inspiration for organic chemists. In this context, one of the most interesting aspects of enzymes is their ability to promote reactions with excellent levels of selectivity, such as chemo-, regio-, and stereoselectivity, which in many cases are difficult to achieve with classical chemical methods.[1] To this end, chemists have been pursuing the synthesis of relatively small molecules that mimic the catalytic properties of enzyme active sites, preferably with increased stability and substrate scope compared to the corresponding enzymes. From this point of view, oligopeptides represent a privileged scaffold since they are made of the same building blocks as enzymes. Moreover, they are easy to synthesize, allowing for rapid catalyst screening through the use of combinatorial techniques.[2] Although they are chemically stable, peptides can be easily degraded and are thus environmentally friendly, which is an additional advantage.

Over the past three decades, peptides have been successfully employed to catalyze a wide range of reactions.[2] For example, Miller and co-workers have investigated the use of peptides made both of natural and nonproteinogenic amino acids to catalyze enantioselective[3] and site-selective[4] processes. One elegant example concerns the kinetic resolution of *trans*-2-*N*-acetamidocyclohexanol **1** through acylation of the alcohol moiety (Scheme 1).[3a−c] Several catalysts, all including an alkylimidazole moiety as the active functional group, were synthesized and tested for catalysis. Catalyst **3**, incorporating an L-proline-Aib sequence (Aib, α-aminoisobutyric acid) known to favor β-turns,[5] catalyzed preferentially the acylation of (*S*,*S*)-**1** with promising selectivity ($k_{(S,S)}/k_{(R,R)}$ = 17). Catalyst **4**, lacking the secondary structure, exhibited no selectivity, showing thus that the selectivity is determined by the secondary structure of the peptide, rather than by the configuration of the α-carbon. Interestingly, catalyst **5**, which incorporates the nonproteinogenic D-proline in a D-Pro-Aib sequence, showed higher selectivity than catalyst **3**, favoring the acylation of the opposite enantiomer ($k_{(R,R)}/k_{(S,S)}$ = 28). It is also worth noting that tetrapeptide **6**, which is an epimer of catalyst **5** at the proline α-carbon, proved to be much less selective, favoring the acylation of the (*S*,*S*) enantiomer ($k_{(S,S)}/k_{(R,R)}$ = 3). The selectivity was later improved further by increasing the catalyst size up to an octapeptide, showing a remarkable k_{rel} of 51.[6] Although significant experimental mechanistic studies have been performed[3b,c,7] (*vide infra*), many details of the reaction mechanism, in particular the origin of the observed enantioselectivity, still remain unclear.

Herein, we present a detailed mechanistic investigation by means of density functional theory (DFT) calculations.[8,9] First, the mechanism of the reaction catalyzed by the small and nonchiral 1,5-dimethylimidazole will be discussed. This is important both to establish the mechanism and to evaluate possible model approximations. Then, the results regarding the substrate acylation step using tetrapeptide **5** as the catalyst will be presented, focusing on the factors governing the enantioselectivity.

Received: September 23, 2015
Revised: November 25, 2015

DOI: 10.1021/acscatal.5b02131
ACS Catal. 2016, 6, 1165−1171

Scheme 1. Kinetic Resolution of *trans*-2-N-Acetamidocyclohexanol 1[3a−c]

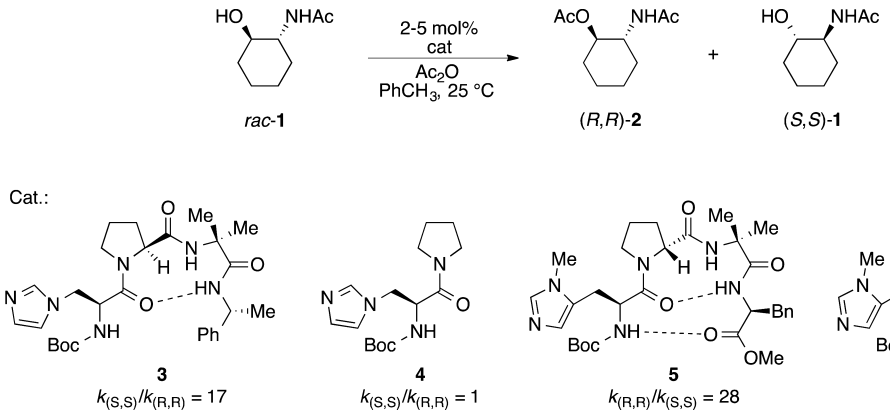

2. COMPUTATIONAL METHODS

All calculations were performed using density functional theory with the B3LYP[10] functional, as implemented in the Gaussian 09 program package.[11] The 6-31G(d,p) basis set was used for geometry optimizations. Final energies for the fully optimized structures were obtained with the larger 6-311+G(2d,2p) basis set. Analytical frequency calculations were carried out at the B3LYP/6-31G(d,p) level to obtain Gibbs free energy corrections at 298 K and to characterize the nature of stationary points. Solvation free energies in toluene (ε = 2.3741) were calculated as single-point corrections on the optimized structures using the SMD solvation model.[12] Dispersion corrections were added using the DFT-D2 method.[13] For comparison, transition state energies were also calculated as single points using the M06 functional[14] with the 6-311+G(2d,2p) basis set (see Supporting Information). Inclusion of dispersion turned out to be critical in order to reproduce the experimentally observed enantioselectivity (the B3LYP energies without dispersion are reported in the Supporting Information). Similar conclusions have been found previously for other reactions.[15] Three-dimensional structures in the figures were generated using CYLview.[16]

3. RESULTS AND DISCUSSION

3.1. Acylation Catalyzed by 1,5-Dimethylimidazole.

First, we investigate the reaction mechanism using 1,5-dimethylimidazole as a small nonchiral model of the catalyst. The calculations confirm that the reaction follows the commonly proposed mechanism, proceeding through two sequential steps, as shown in Scheme 2. This mechanism is very similar to the acylation reaction catalyzed by CF_3−PIP[9b] and 4-(dimethylamino)pyridine.[9a] In the first step, 1,5-dimethylimidazole reacts with acetic anhydride, affording the *N*-acetyl-1,5-dimethylimidazolium cation and acetate. In the second step, the alcohol attacks the carbonyl of the *N*-acetyl-1,5-dimethylimidazolium ion, concertedly with the acetate abstracting the proton from the alcohol. The dissociation of the acetyl group from the catalyst occurs also in the same step. The calculated free energy profile is shown in Figure 1 and the optimized structures in Figures 2 and 3.

It is interesting to note that the calculations indicate that the first step can occur with or without the assistance of substrate **1** (through **TS1′** and **TS1**, respectively). In the first case, the reaction barrier is slightly lower (15.0 vs 18.2 kcal/mol), but the resulting intermediate **Int′** is slightly higher in energy compared to the corresponding intermediate **Int** that does not include the substrate (+9.5 vs +11.7 kcal/mol relative to the reactants).

For the second step, several transition state geometries exist. The main differences concern which face of the amidic carbonyl

Scheme 2. General Reaction Mechanism for Alcohol Acylation Catalyzed by Substituted Imidazole

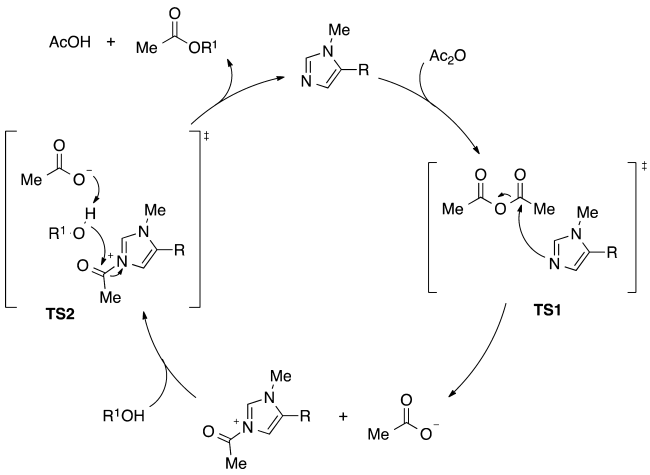

is attacked by the nucleophilic alcohol (*Re* or *Si*), which one of the C−H moieties of the imidazole (C2 or C4) is interacting with the acetate, and finally the relative orientation of the substrate N−H relative to the adjacent endocyclic C−H (*syn* or *anti*). This gives rise to eight possible transition states (see optimized structures in Figure 3). The lowest energy TS is **TS2**$_{\text{Re-C2-anti}}$ (**TS2** in Figure 1), and it is only 4.5 kcal/mol higher than **Int**, i.e., 14.0 kcal/mol relative to the reactants.

An important finding here is that the transition states with an *anti* orientation between adjacent N−H and C−H groups in the substrate are always associated with lower energies (by at least 5 kcal/mol) compared to the corresponding ones with a *syn* orientation. One reason for this is that in the TSs with a *syn* orientation, the amide has to deviate from planarity (by ca. 15°) in order to form a hydrogen bond to the acetyl group, while this is not necessary for TSs with an *anti* conformation. Indeed, a distortion-interaction analysis of a *syn*−*anti* pair of transition states confirms that the distortion energy of alcohol **1** is much greater for the *syn* transition state compared to the *anti* counterpart (see details in the Supporting Information).

3.2. Acylation Catalyzed by Tetrapeptide.

The calculations above for the reaction mechanism using 1,5-dimethylimidazole as the catalyst suggest that the first step could occur with or without the assistance of the substrate. The calculated energy difference between the two transition states (**TS1** and **TS1′**), and also between the resulting intermediates (**Int** and **Int′**), is quite small, and it is therefore not possible to

DOI: 10.1021/acscatal.5b02131
ACS Catal. 2016, 6, 1165−1171

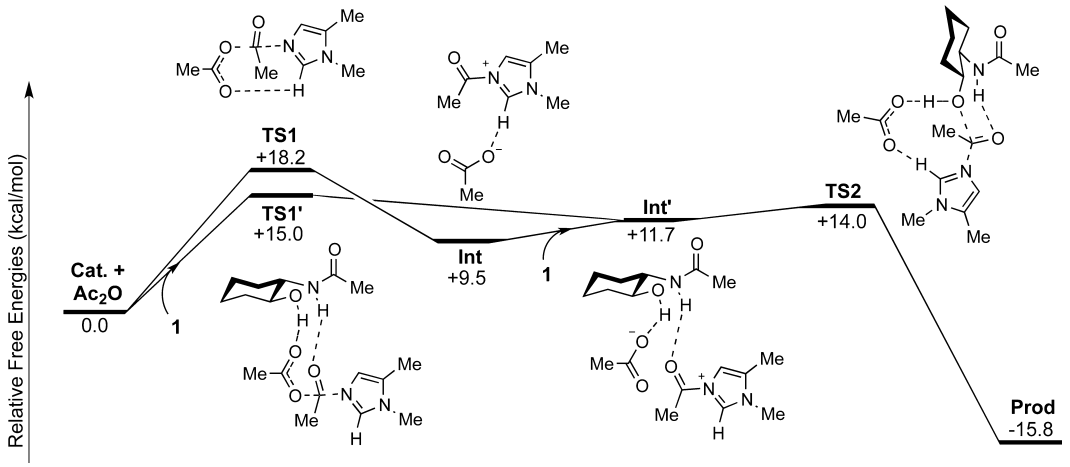

Figure 1. Free energy profile for the acylation of (*R*,*R*)-**1** catalyzed by 1,5-dimethylimidazole.

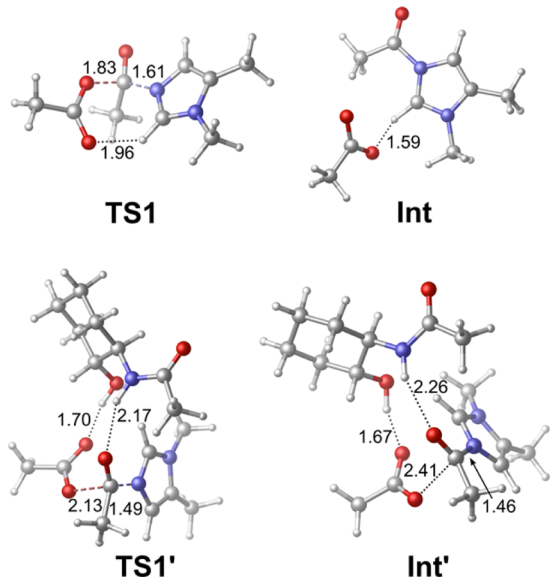

Figure 2. Optimized structures of transition states and intermediates for the acyl transfer to 1,5-dimethylimidazole. Distances are given in Ångströms.

rule out either of them, especially considering the potential errors associated with the calculation of the entropic contributions.

The situation is likely to be the same for the tetrapeptide case, i.e., that the first step can occur with or without the involvement of the alcohol substrate. One possible complication for the investigation of the origins of the enantioselectivity of the kinetic resolution might come from the presence of two diastereomeric forms of **TS1**′, depending on which enantiomer of the substrate is involved in the reaction, and that the first step might therefore contribute to the enantioselectivity. However, it is chemically reasonable to assume that **Int** and **Int**′ are in rapid equilibrium, i.e., that the alcohol moiety can rapidly dissociate from the intermediate structure, and that **TS2** therefore can be assumed to be the selectivity-determining step. This assumption is supported by an important piece of experimental information. Namely, Miller and co-workers have synthesized an analogue of the tetrapeptide catalyst in which the amide bond between proline and Aib is substituted for an olefin.[7] The structure in solution was found to be very similar to that of the parent tetrapeptide. Very importantly, however, when used as a catalyst for the same kinetic resolution reaction, the modified catalyst showed no selectivity.[7] These experiments demonstrate thus that this amide group plays an important role in the selectivity-determining step. Since it is located quite far from the imidazole ring, it is hard to imagine how the amide group could affect the acylation step (**TS1**). It is, on the other hand, directly involved in the transition state for the second step (**TS2**), as can be seen from the optimized transition state structures below.

For these reasons, we have in this section decided to model only the second step of the reaction with tetrapeptide **5** as the catalyst. Moreover, the fact that large energy differences are found in the small model between transition states with *anti* and *syn* orientations suggests that it is sufficient to only consider the transition states with *anti* orientations in the full catalyst calculations.

NMR studies have established that in the reaction conditions used in the experiments, tetrapeptide **5** assumes only one conformation in which two hydrogen bonds are formed to give a stable *β*-hairpin structure (see Figure 4).[3b] The existence of these two hydrogen bonds restricts thus the conformational space of the catalyst. However, the imidazole part is unconstrained and can rotate to generate different conformations during the acylation. There are three main rotatable bonds, marked with letters A, B, and C in Figure 4 (see the Supporting Information for full details). Given that the rotation around bond A generates three possibilities (A1, A2, and A3), while the rotations around bonds B and C give rise to two possibilities each (B1 and B2, C1 and C2), there are 12 possible conformers of the acylated catalyst. It should moreover be considered that the nucleophile can attack the *N*-acetyl group on either *Re* or *Si* faces, which results thus in a total of 24 TSs that have to be considered. Finally, all these possibilities have to be studied for the two enantiomeric substrates, resulting in 48 transition states.[17] We have optimized all these transition states and evaluated their relative free energies. The results are listed in Table 1.

Scrutiny of the optimized transition state geometries indicates that they can be classified into three groups on the basis of their interaction mode between the acylated catalyst, the substrate, and the acetate (see Figure 4). In "Mode I," the peptide donates a hydrogen bond from the amide bond between proline and *α*-aminoisobutyric acid to the substrate

DOI: 10.1021/acscatal.5b02131
ACS Catal. 2016, 6, 1165−1171

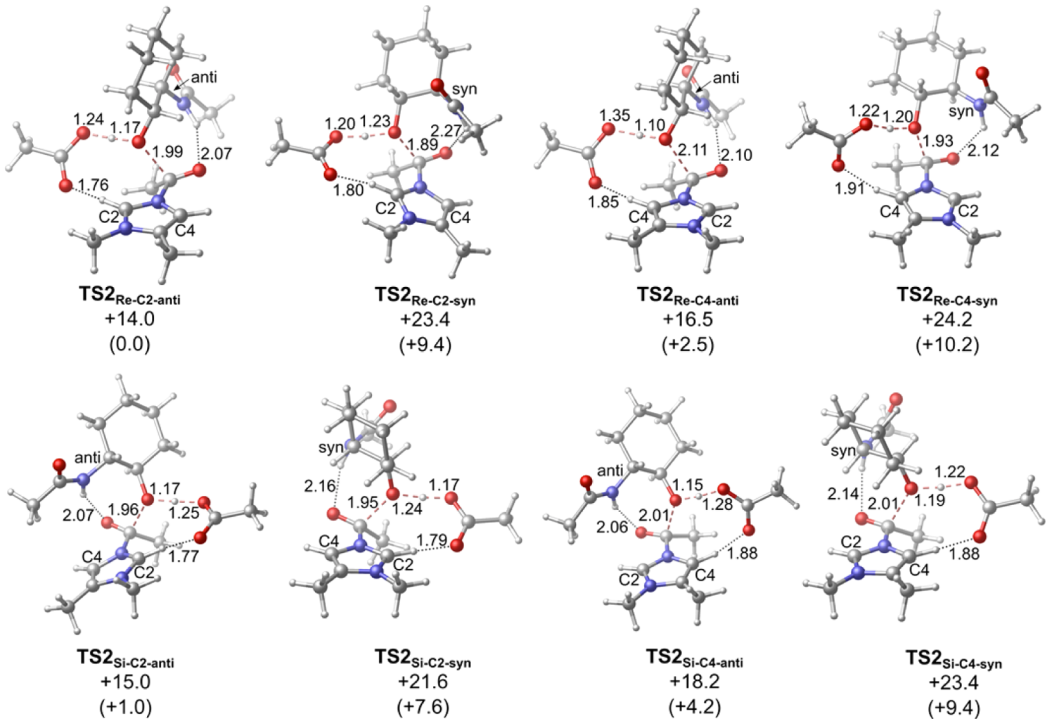

Figure 3. Optimized structures of the eight possible transition states for the acyl transfer from 1,5-dimethylimidazole to (*R*,*R*)-**1**. Energies relative to the isolated catalyst and reactants are given in kcal/mol. Energy values in parentheses are relative to $\mathbf{TS2}_{\text{Re-C2-anti}}$, which corresponds to **TS2** in Figure 1.

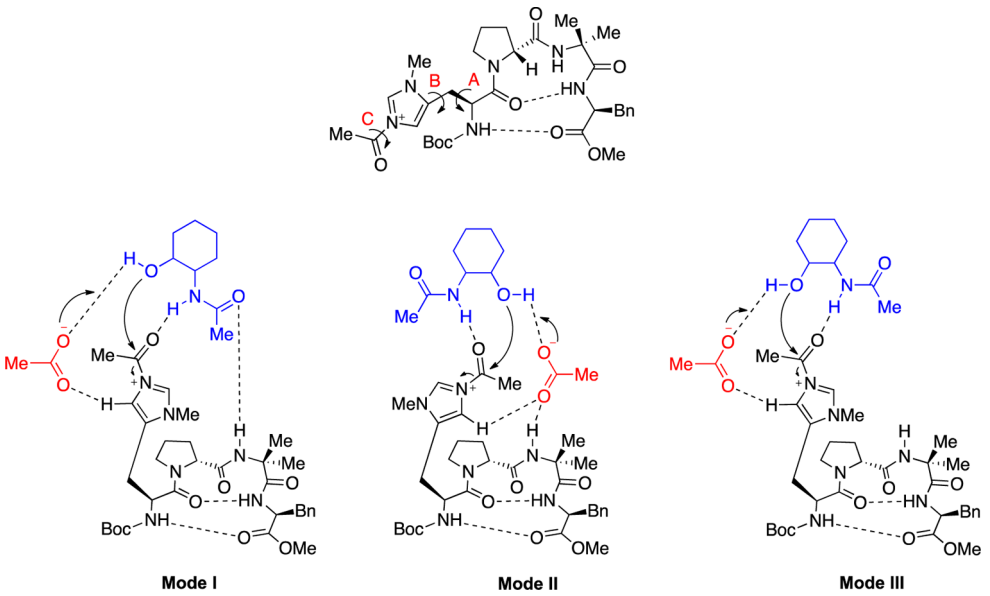

Figure 4. Representation of the possible conformational variables in the full model N-acylated catalyst and of the three interaction modes between catalyst, substrate, and acetate anion.

amide carbonyl oxygen. This interaction was previously proposed by Miller and co-workers.[7] In "Mode II," the same amidic NH from the peptide is hydrogen-bonded to the acetate anion instead. Finally, in "Mode III," no hydrogen bond is formed between the peptide and the reacting groups. The lowest energy transition states for the reaction occurring on the two enantiomers through the three interaction modes are presented in Figure 5. Figures of all other TSs are given in the Supporting Information.

The energy difference between the lowest energy transition states leading to the acylation of the two enantiomers (**A1B1C2*Si*** and **A1B2C2*Re*** for the acylation of (*R*,*R*)-**1** and (*S*,*S*)-**1**, respectively) is 2.6 kcal/mol, favoring the acylation of the (*R*,*R*)-enantiomer. Experimental studies showed that the relative acylation rate of (*R*,*R*)-**1** and (*S*,*S*)-**1** is 28,[3b] which can be converted to a difference in energy barriers of 2.0 kcal/mol using classical transition state theory. The calculations are thus in very good agreement with the experimental results.[18]

DOI: 10.1021/acscatal.5b02131
ACS Catal. 2016, 6, 1165−1171

Table 1. Calculated Relative Free Energies (kcal/mol) of Transition States for the Acylation of (*R*,*R*)-1 and (*S*,*S*)-1

	(*R*,*R*)-**1**		(*S*,*S*)-**1**	
TS	Mode	$\Delta\Delta G^{\ddagger}$	Mode	$\Delta\Delta G^{\ddagger}$
A1B1C1*Si*	III	5.5	III	5.2
A2B1C1*Si*	III	3.9	III	4.6
A3B1C1*Si*	III	6.0	III	5.8
A1B2C1*Si*	III	5.6	III	2.7
A2B2C1*Si*	III	6.4	III	4.8
A3B2C1*Si*	I	1.4	I	9.2
A1B1C2*Si*	I	**0.0**	III	3.0
A2B1C2*Si*	III	5.6	III	8.6
A3B1C2*Si*	I	1.3	I	3.5
A1B2C2*Si*	II	7.6	II	6.0
A2B2C2*Si*	III	6.8	III	6.9
A3B2C2*Si*	III	7.1	III	6.9
A1B1C1*Re*	III	4.5	III	7.7
A2B1C1*Re*	III	5.8	III	4.0
A3B1C1*Re*	III	4.1	III	8.1
A1B2C1*Re*	III	7.3	III	5.2
A2B2C1*Re*	III	5.2	III	4.3
A3B2C1*Re*	III	3.9	III	4.7
A1B1C2*Re*	III	6.1	III	6.8
A2B1C2*Re*	III	8.0	III	7.4
A3B1C2*Re*	II	5.3	II	6.5
A1B2C2*Re*	II	2.4	II	2.6
A2B2C2*Re*	III	7.4	converges to **A1B2C2*Re***	
A3B2C2*Re*	III	10.3	III	8.5

By analysis of the interactions in the various transition state structures, one can uncover the factors that govern the stereoselectivity of the process. The lowest energy TS leading to the acylation of the (*R*,*R*)-enantiomer (**A1B1C2*Si***) adopts interactions according to "Mode I", i.e., the catalyst donates one hydrogen bond to the substrate amide carbonyl. The lowest energy TS leading to the acylation of (*S*,*S*)-**1** is **A1B2C2*Re***, which belongs to "Mode II" TSs (see Figure 5). When comparing the lowest energy "Mode I"-transition states leading to the acylation of the two enantiomers (Figures 5 and 6), it is clear that in the TS leading to (*R*,*R*)-**1** acylation there is one additional stabilizing interaction. The amidic N−H of the substrate interacts with the imidazole-bound acetyl group. This additional interaction exists also in other low-lying "Mode I" (*R*,*R*)-**1** acylation transition states (**A3B2C1*Si*** and **A3B1C2*Si***), where it can favor the acylation by stabilizing the developing negative charge during the nucleophilic attack. It is noteworthy that this interaction cannot be found in any of the TSs adopting "Mode I"-interaction leading to the acylation of (*S*,*S*)-**1**. In the lowest energy TS leading to the acylation of (*S*,*S*)-**1** (**A1B2C2*Re***, Figure 5), which belongs to "Mode II" TSs, the substrate amide can donate a hydrogen bond to the imidazole-bound acetate, thus stabilizing the nucleophilic attack. However, the substrate cannot accept any hydrogen bond from the peptide. Instead, the amide bond between proline and α-aminoisobutyric acid donates a hydrogen bond to the acetate anion (as in all "Mode II"-transition states). These differences in the interaction modes, in particular the existence of an additional hydrogen bond in the lowest energy TSs leading to the acylation of (*R*,*R*)-**1**, are suggested to govern the stereoselectivity of the process. "Mode III"-transition states do not have any hydrogen bonds between the peptide and the reaction center and are generally associated with higher energy

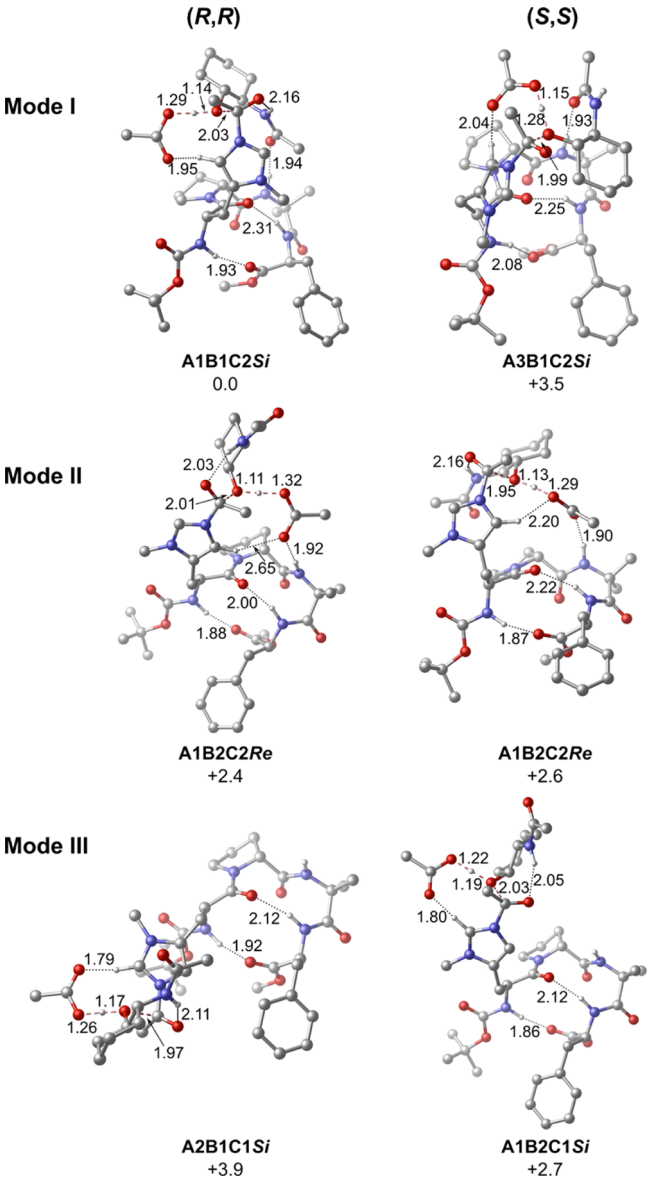

Figure 5. Lowest energy transition states for the three interaction modes for the reaction occurring on the two enantiomers. All carbon-bound hydrogen atoms, with the exception of those involved in hydrogen bonds, are omitted for clarity. Relative energies (in kcal/mol) are indicated.

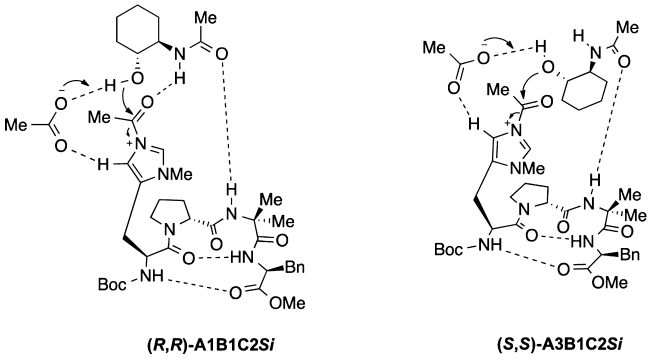

Figure 6. Schematic representation of the lowest energy "Mode I"-transition states for the reaction occurring on the two enantiomers.

DOI: 10.1021/acscatal.5b02131
ACS Catal. 2016, 6, 1165−1171

barriers. There are, however, a few exceptions. The lowest energy "Mode III"-TS leading to (*S*,*S*)-**1** acylation (**A1B2C1*Si***) has very similar energy to the lowest "Mode II"-TS. Also in this case, the substrate-amide N−H interacts with the electrophilic acetyl group stabilizing the nucleophilic attack.

Finally, one technical detail should be mentioned here. For comparison, we have performed single-point calculations using the M06 functional[14] on the B3LYP optimized geometries (see Supporting Information). The results are very similar to those obtained with the B3LYP-D2 method, with the (*R*,*R*)-**1** acylation being favored over the (*S*,*S*)-**1** acylation by 1.6 kcal/mol. Analysis of the interaction modes in the lowest energy transition states leads to the same conclusions concerning the factors governing the enantioselectivity.

4. CONCLUSIONS

In summary, the calculations presented here offer an important basis for understanding the origins of the stereoselectivity in the kinetic resolution of *trans*-2-*N*-acetamidocyclohexanol by a tetrapeptide-catalyzed acylation. The calculations reproduce the experimentally observed stereoselectivity, and by considering all possible conformers and calculating a large number of transition states, it is possible to elucidate the main factors that govern the stereoselectivity. The tetrapeptide recognizes the (*R*,*R*) substrate by donating a hydrogen bond to the substrate amide group, which at the same time is hydrogen bonded to the *N*-acetyl group during the acylation. This kind of interaction mode is only accessible for the (*R*,*R*) substrate. The alternative interaction modes are associated with higher energy barriers. These findings might aid the understanding of peptide-catalyzed kinetic resolution of other substrates and also in the design of new catalytic systems. However, due to the large number of transition states that have to be considered, the effect of possible catalyst modifications are not easy to predict without detailed calculations, as a small change in one parameter can influence other aspects of the catalyst-substrate interactions and lead to large energy differences.

■ ASSOCIATED CONTENT

Supporting Information

The Supporting Information is available free of charge on the ACS Publications website at DOI: 10.1021/acscatal.5b02131.

Distortion-interaction analysis, conformer definition of tetrapeptide catalyst, geometrical features of optimized transition states for tetrapeptide catalyst, relative transition state energies for tetrapeptide catalyst with different functionals, and structures and Cartesian coordinates of optimized stationary points (PDF)

■ AUTHOR INFORMATION

Corresponding Authors

*E-mail: rongzhen@hust.edu.cn.
*E-mail: stefano.santoro@unipg.it.
*E-mail: fahmi.himo@su.se.

Notes

The authors declare no competing financial interest.

■ ACKNOWLEDGMENTS

This work was supported by the National Natural Science Foundation of China (21503083), startup funding from Huazhong University of Science and Technology, the Swedish Research Council, the Göran Gustafsson Foundation, and the Knut and Alice Wallenberg Foundation. Computer time was generously provided by the Swedish National Infrastructure for Computing. We thank Prof. Jeremy Harvey for valuable discussions.

■ REFERENCES

(1) (a) Faber, K. *Biotransformations in Organic Chemistry*, 6th ed.; Springer-Verlag: New York, 2011. (b) Drauz, K.; Gröger, H.; May, O. *Enzyme Catalysis in Organic Synthesis*, 3rd ed.; Wiley-VCH Verlag: Weinheim, 2012.

(2) For selected reviews, see: (a) Miller, S. J. *Acc. Chem. Res.* **2004**, *37*, 601−610. (b) Davie, E. A. C.; Mennen, S. M.; Xu, Y.; Miller, S. J. *Chem. Rev.* **2007**, *107*, 5759−5812. (c) Freund, M.; Tsogoeva, S. B. Peptides for asymmetric catalysis. In *Catalytic Methods in Asymmetric Synthesis: Advanced Materials, Techniques, and Applications*; Gruttadauria, M., Giacalone, F., Eds.; John Wiley & Sons, Inc.: Hoboken, NJ, 2011; pp 529−578. (d) Wennemers, H. *Chem. Commun.* **2011**, *47*, 12036−12041.

(3) For selected examples, see: (a) Miller, S. J.; Copeland, G. T.; Papaioannou, N.; Horstmann, T. E.; Ruel, E. M. *J. Am. Chem. Soc.* **1998**, *120*, 1629−1630. (b) Copeland, G. T.; Jarvo, E. R.; Miller, S. J. *J. Org. Chem.* **1998**, *63*, 6784−6785. (c) Jarvo, E. R.; Copeland, G. T.; Papaioannou, N.; Bonitatebus, P. J., Jr.; Miller, S. J. *J. Am. Chem. Soc.* **1999**, *121*, 11638−11643. (d) Sculimbrene, B. R.; Morgan, A. J.; Miller, S. J. *Chem. Commun.* **2003**, 1781−1785. (e) Lewis, C. A.; Chiu, A.; Kubryk, M.; Balsells, J.; Pollard, D.; Esser, C. K.; Murry, J.; Reamer, R. A.; Hansen, K. B.; Miller, S. J. *J. Am. Chem. Soc.* **2006**, *128*, 16454−16455. (f) Lewis, C. A.; Gustafson, J. L.; Chiu, A.; Balsells, J.; Pollard, D.; Murry, J.; Reamer, R. A.; Hansen, K. B.; Miller, S. J. *J. Am. Chem. Soc.* **2008**, *130*, 16358−16365. (g) Fiori, K. W.; Puchlopek, A. L. A.; Miller, S. J. *Nat. Chem.* **2009**, *1*, 630−634. (h) Gustafson, J.; Lim, D.; Miller, S. J. *Science* **2010**, *328*, 1251−1255.

(4) For selected examples, see: (a) Griswold, K. S.; Miller, S. J. *Tetrahedron* **2003**, *59*, 8869−8875. (b) Lewis, C. A.; Miller, S. J. *Angew. Chem., Int. Ed.* **2006**, *45*, 5616−5619. (c) Jordan, P. A.; Miller, S. J. *Angew. Chem., Int. Ed.* **2012**, *51*, 2907−2911. (d) Pathak, T. P.; Miller, S. J. *J. Am. Chem. Soc.* **2012**, *134*, 6120−6123.

(5) (a) Zimmerman, S. S.; Scheraga, H. A. *Biopolymers* **1977**, *16*, 811−843. (b) Rose, G. D.; Glerasch, L. M.; Smith, J. A. *Adv. Protein Chem.* **1985**, *37*, 1−109.

(6) Jarvo, E. R.; Vasbinder, M. M.; Miller, S. J. *Tetrahedron* **2000**, *56*, 9773−9779.

(7) Vasbinder, M. M.; Jarvo, E. R.; Miller, S. J. *Angew. Chem., Int. Ed.* **2001**, *40*, 2824−2827.

(8) For a review on organocatalytic acylations from a computational perspective, see: Larionov, E.; Zipse, H. *Wires Comput. Mol. Sci.* **2011**, *1*, 601−619.

(9) For selected examples of computational mechanistic investigations on amine-catalyzed acylations, see: (a) Xu, S.; Held, I.; Kempf, B.; Mayr, H.; Steglich, W.; Zipse, H. *Chem. - Eur. J.* **2005**, *11*, 4751−4757. (b) Li, X.; Liu, P.; Houk, K. N.; Birman, V. B. *J. Am. Chem. Soc.* **2008**, *130*, 13836−13837. (c) Shinisha, C. B.; Sunoj, R. B. *Org. Lett.* **2009**, *11*, 3242−3245. (d) Larionov, E.; Mahesh, M.; Spivey, A. C.; Wei, Y.; Zipse, H. *J. Am. Chem. Soc.* **2012**, *134*, 9390−9399. (e) Nishino, R.; Furuta, T.; Kan, K.; Sato, M.; Yamanaka, M.; Sasamori, T.; Tokitoh, N.; Kawabata, T. *Angew. Chem., Int. Ed.* **2013**, *52*, 6445−6449.

(10) (a) Becke, A. D. *J. Chem. Phys.* **1993**, *98*, 5648−5652. (b) Lee, C.; Yang, W.; Parr, R. G. *Phys. Rev. B: Condens. Matter Mater. Phys.* **1988**, *B37*, 785−789.

(11) Frisch, M. J.; Trucks, G. W.; Schlegel, H. B.; Scuseria, G. E.; Robb, M. A.; Cheeseman, J. R.; Scalmani, G.; Barone, V.; Mennucci, B.; Petersson, G. A.; Nakatsuji, H.; Caricato, M.; Li, X.; Hratchian, H. P.; Izmaylov, A. F.; Bloino, J.; Zheng, G.; Sonnenberg, J. L.; Hada, M.; Ehara, M.; Toyota, K.; Fukuda, R.; Hasegawa, J.; Ishida, M.; Nakajima, T.; Honda, Y.; Kitao, O.; Nakai, H.; Vreven, T.; Montgomery, J. A., Jr.; Peralta, J. E.; Ogliaro, F.; Bearpark, M.; Heyd, J. J.; Brothers, E.; Kudin, K. N.; Staroverov, V. N.; Kobayashi, R.; Normand, J.; Raghavachari, K.;

DOI: 10.1021/acscatal.5b02131
ACS Catal. 2016, 6, 1165−1171

Rendell, A.; Burant, J. C.; Iyengar, S. S.; Tomasi, J.; Cossi, M.; Rega, N.; Millam, J. M.; Klene, M.; Knox, J. E.; Cross, J. B.; Bakken, V.; Adamo, C.; Jaramillo, J.; Gomperts, R.; Stratmann, R. E.; Yazyev, O.; Austin, A. J.; Cammi, R.; Pomelli, C.; Ochterski, J. W.; Martin, R. L.; Morokuma, K.; Zakrzewski, V. G.; Voth, G. A.; Salvador, P.; Dannenberg, J. J.; Dapprich, S.; Daniels, A. D.; Farkas, O.; Foresman, J. B.; Ortiz, J. V.; Cioslowski, J.; Fox, D. J. *Gaussian 09*, revision B.01; Gaussian, Inc.: Wallingford, CT, 2010.

(12) Marenich, A. V.; Cramer, C. J.; Truhlar, D. G. *J. Phys. Chem. B* **2009**, *113*, 6378−6396.

(13) Grimme, S. *J. Comput. Chem.* **2006**, *27*, 1787−1799.

(14) Zhao, Y.; Truhlar, D. G. *Acc. Chem. Res.* **2008**, *41*, 157−167.

(15) For examples, see: (a) Minenkov, Y.; Occhipinti, G.; Jensen, V. R. *J. Phys. Chem. A* **2009**, *113*, 11833−11844. (b) Siegbahn, P. E. M.; Blomberg, M. R. A.; Chen, S.-L. *J. Chem. Theory Comput.* **2010**, *6*, 2040−2044. (c) Harvey, J. N. *Faraday Discuss.* **2010**, *145*, 487−505. (d) McMullin, C. L.; Jover, J.; Harvey, J. N.; Fey, N. *Dalton Trans* **2010**, *39*, 10833−10836. (e) Lonsdale, R.; Harvey, J. N.; Mulholland, A. J. *J. Phys. Chem. Lett.* **2010**, *1*, 3232−3237. (f) Osuna, S.; Swart, M.; Solà, M. *J. Phys. Chem. A* **2011**, *115*, 3491−3496. (g) Ahlquist, M. S. G.; Norrby, P.-O. *Angew. Chem., Int. Ed.* **2011**, *50*, 11794−11797. (h) Santoro, S.; Liao, R.-Z.; Himo, F. *J. Org. Chem.* **2011**, *76*, 9246−9252. (i) Xu, X.; Liu, P.; Lesser, A.; Sirois, L. E.; Wender, P. A.; Houk, K. N. *J. Am. Chem. Soc.* **2012**, *134*, 11012−11025. (j) Huang, G.; Xia, Y.; Sun, C.; Li, J.; Lee, D. *J. Org. Chem.* **2013**, *78*, 988−995. (k) Fadda, E.; Woods, R. J. *Can. J. Chem.* **2013**, *91*, 859−865.

(16) Legault, C. Y. *CYLview*, 1.0b; Université de Sherbrooke: Sherbrooke, Quebec, Canada, 2009. http://www.cylview.org.

(17) The rotation of the phenyl ring of phenylalanine has also been considered. Only the conformer with the lowest energy is presented here.

(18) Boltzmann averaging of all TS energies gives very similar results, with the acylation of (*R*,*R*)-**1** being favored by 2.1 kcal/mol over the acylation of the other enantiomer.

DOI: 10.1021/acscatal.5b02131
ACS Catal. 2016, 6, 1165−1171